This article was downloaded by:
On: *25 January 2011*
Access details: *Access Details: Free Access*
Publisher *Taylor & Francis*
Informa Ltd Registered in England and Wales Registered Number: 1072954 Registered office: Mortimer House, 37-41 Mortimer Street, London W1T 3JH, UK

Separation Science and Technology
Publication details, including instructions for authors and subscription information:
http://www.informaworld.com/smpp/title~content=t713708471

Flow Parameter Profiles in the Crossflow of a Two-Component Fluid through Semipermeable Membranes

S. Avlonitis[a]; D. Papanikas[a]
[a] FLUID MECHANICS LABORATORY DEPARTMENT OF MECHANICAL ENGINEERING, UNIVERSITY OF PATRAS, PATRAS, GREECE

To cite this Article Avlonitis, S. and Papanikas, D.(1997) 'Flow Parameter Profiles in the Crossflow of a Two-Component Fluid through Semipermeable Membranes', Separation Science and Technology, 32: 5, 939 — 950
To link to this Article: DOI: 10.1080/01496399708000937
URL: http://dx.doi.org/10.1080/01496399708000937

PLEASE SCROLL DOWN FOR ARTICLE

Full terms and conditions of use: http://www.informaworld.com/terms-and-conditions-of-access.pdf

This article may be used for research, teaching and private study purposes. Any substantial or systematic reproduction, re-distribution, re-selling, loan or sub-licensing, systematic supply or distribution in any form to anyone is expressly forbidden.

The publisher does not give any warranty express or implied or make any representation that the contents will be complete or accurate or up to date. The accuracy of any instructions, formulae and drug doses should be independently verified with primary sources. The publisher shall not be liable for any loss, actions, claims, proceedings, demand or costs or damages whatsoever or howsoever caused arising directly or indirectly in connection with or arising out of the use of this material.

SEPARATION SCIENCE AND TECHNOLOGY, 32(5), pp. 939–950, 1997

Flow Parameter Profiles in the Crossflow of a Two-Component Fluid through Semipermeable Membranes

S. AVLONITIS* and D. PAPANIKAS
FLUID MECHANICS LABORATORY
DEPARTMENT OF MECHANICAL ENGINEERING
UNIVERSITY OF PATRAS
PATRAS, GREECE

Downloaded At: 11:38 25 January 2011

ABSTRACT

The analytical solution for spiral-wound module performance is a useful tool for developing explicit equations for the local values of variables like effective pressure, water flux, salt wall concentration, and velocities for seawater feed solutions. Depending on the operating conditions, knowledge of the local values of these variables could be useful to predict possible areas on the membrane surface where scale formation or fouling is likely to occur. Reasonable values for all variables have been found by using the developed equations at any point in the permeate and the feed side of the membrane. Although the method has been applied for spiral wound reverse osmosis membranes, it is believed that the same method could be used in similar hydrodynamic situations where flow through porous media is taking place.

Key Words. Membranes; Reverse osmosis; Crossflow; Spiral wound modules; Velocity-effective pressure-flux-concentration profiles

INTRODUCTION

In spiral-wound reverse osmosis membranes a two-component fluid, which is a salt water solution, travels along the membrane. The water can

* To whom correspondence should be addressed at his present address: Miriofitou 16, Amfiali 18757, Greece.

Copyright © 1997 by Marcel Dekker, Inc.

pass through the membrane perpendicular to the direction of the solution flow, while the salt is rejected. The size of the spiral wound modules and the local production of permeate causes significant changes in effective pressure, water flux, velocities, and salt concentration in this type of modules. A knowledge of the profiles of these variables could be useful to predict the area on the membrane surface where salt precipitation is more likely to take place. On the other hand, a very detailed description of the module performance is always useful to suggest optimum operating conditions or a tapered configuration. Since one of the assumptions in this analysis is flow through porous media, similar results could be obtained in other flow situations where crossflow of one component takes place in a multicomponent fluid.

Taking into account the two-dimensional character of the flow situation, Berman (3) developed a velocity profile for laminar and steady flow between parallel flat sheet membranes with constant permeate flux. Other equations for the velocity profile have been suggested by Rocco (4) and Miyoshi et al. (5). Battacharyya et al. (6) used a numerical method to determine some of the flow profiles at low feed concentrations. Although different numerical methods can be used to determine the above-mentioned profiles, an analytical procedure is always more attractive since it is a straightforward procedure.

Downloaded At: 11:38 25 January 2011

THEORY

The modeling of spiral-wound modules is based on material balances for the solvent and the solute in the permeate and the brine channels and Darcy's law (see Eqs. 1 to 5). The problem of formulating the flow conditions in these modules can be accomplished only after several assumptions are made. These assumptions are presented in Table 1. The flow has been considered laminar and steady, and average values of velocities have been used. A more detailed analysis for the formulation of module performance has been published (1, 2). The element volume for which the equations have been applied is given in Fig. 1.

$$\frac{\partial u_p(x, y)}{\partial y} = \frac{2J(x, y)}{h_p} \tag{1}$$

$$\frac{\partial \Delta P_{ef}(x, y)}{\partial y} = -\frac{dP_p(x, y)}{dy} = k_{fp}\mu u_p(x, y) \tag{2}$$

$$\frac{\partial u_b(x, y)}{\partial x} = -\frac{2J(x, y)}{h_b} \tag{3}$$

TABLE 1
Assumptions for the 2-Dimension Calculations

1. Validity of Darcy's law for permeate and brine channel. Flow through porous media has been assumed; see Eqs. (2) and (4).
2. Validity of solution-diffusion model for the transport of water through the membrane. The water flux is given at any point on membrane surface by

$$J(x, y) = k_1 \Delta P_{ef}(x, y) \tag{A.1}$$

3. No flow restrictions for the locally produced permeate in the porous substructure of the asymmetric or composite membrane.
4. The permeate concentration has been neglected in comparison to the feed concentration.
5. The module is made up of flat channels with a constant geometrical shape; see Table 2.
6. Constant fluid properties.
7. Negligible diffusive mass transport along the x and y direction in both channels. This means that the flux through the membrane due to diffusion is much smaller than the flux due to convection. The driving force for water transport is the effective pressure across the membrane.
8. The brine concentration varies linearly with the distance L, in the axial direction.

$$c_b(x) = c_f + fx \tag{A.2}$$

where

$$f = \frac{c_b(L) - c_f}{L}$$

The value of f is an indication of the recovery ratio R. Detailed studies of the R.O. modules' performance with experimental and theoretical data (7) have shown that this assumption is realistic for seawater membranes at normal operating conditions, $R < 10\%$, and for brackish water membranes. In the theoretical situation where a high recovery ratio is taking place for seawater membranes, Eq. (A.2) causes serious errors in predictions of the working equations.

9. Validity of the thin film theory, with the approximation given by

$$c_{bw}(x, y) = c_b(x, y)\left(1 + \frac{J(x, y)}{k}\right) \tag{A.3}$$

10. As has been shown in Ref. 3, the mass transfer coefficient depends strongly on the flow conditions and the properties of the feed solution. Both factors vary at every point on the membrane surface, resulting in different mass transfer coefficient values. However, in this analysis a constant mass transfer coefficient value at any point on the membrane surface has been assumed.
11. Osmotic pressure proportional to the concentration:

$$\pi(x, y) = \omega c_{bw}(x, y) \tag{A.4}$$

Downloaded At: 11:38 25 January 2011

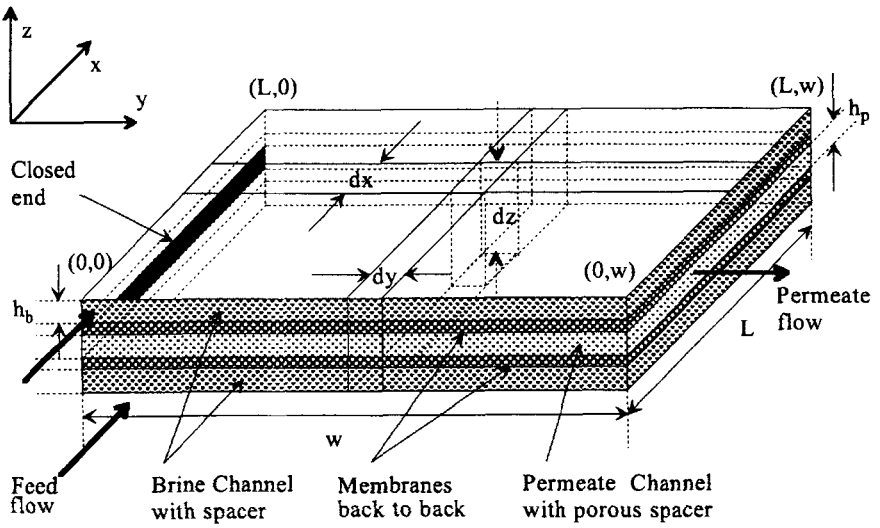

FIG. 1 Unwound module.

$$\frac{\partial[\Delta P_{ef}(x, y) + \pi_{bw}(x, y)]}{\partial x} = \frac{dP_b(x, y)}{dx} = -k_{fb}\mu u_b(x, y) \tag{4}$$

$$\frac{\partial c_b(x, y)}{\partial x} = \frac{2J(x, y)}{u_b(x, y)h_b}[c_b(x, y) - c_p(x, y)] \tag{5}$$

By using the assumptions and equations in Table 1 and the differential Eqs. (1) to (5), after integration over the surface area of the module, the effective pressure profile has been found to be given by Eq. (6). If Eq. (6) is multiplied by the water permeability coefficient k_1, then the water flux at any point on the membrane surface will be given by Eq. (7).

$$\Delta P_{ef}(x, y) = k\frac{\Delta P - c_f\omega + \dfrac{c_f u_f k_{fb}\mu}{f}\ln\dfrac{c_f}{c_f + fx} - \omega fx\cosh\dfrac{y}{q}}{k + k_1\omega(c_f + fx)}\Big/\cosh\frac{W}{q} \tag{6}$$

$$J(x, y) = k\frac{\Delta P - c_f\omega + \dfrac{c_f u_f k_{fb}\mu}{f}\ln\dfrac{c_f}{c_f + fx} - \omega fx\cosh\dfrac{y}{q}}{\dfrac{k}{k_1} + \omega(c_f + fx)}\Big/\cosh\frac{W}{q} \tag{7}$$

where $\Delta P = [P_b(0, w) - P_p(0, w)]$

Downloaded At: 11:38 25 January 2011

The validity of Eq. (7) has been tested elsewhere (2, 7), not only by the authors' experimental data but also by Taniguchi (10). A very good agreement was found with the results given by other analytical and numerical models (8–10).

A combination of Eqs. (A.1), (A.3), and (7) will result in the final Eq. (8) for the salt wall concentration.

$$c_{bw}(x, y) = [c_f + fx]\left(1 + \frac{J(x, y)}{k}\right) \tag{8}$$

The brine velocity profile can be found by integration of Eq. (3) by the use of Eqs. (A.1) and (7). This leads to

$$\begin{aligned} u_b(x, y) = u_f &- \frac{2k \cosh\left(\frac{y}{q}\right)}{\omega f h_b \cosh\left(\frac{w}{q}\right)} \\ &\times \left[(\Delta P - c_f\omega) \ln \frac{k + k_1\omega(c_f + fx)}{k + k_1\omega c_f} - \omega fx + \frac{c_f u_f k_{fb}\mu}{f}\right] \\ &\times \left[\frac{k_1\omega fx}{k}\right. \\ &\left. - \ln \frac{c_f + fx}{c_f} \ln \frac{k + k_1\omega(c_f + fx)}{k} - \frac{k_1^2\omega^2}{4k^2}(f^2x^2 + 2c_f fx)\right] \\ &+ \left[\frac{k + k_1\omega c_f}{k_1} \ln \frac{k + k_1\omega(c_f + fx)}{k + k_1\omega c_f}\right] \end{aligned} \tag{9}$$

If the same procedure is applied for Eq. (1), then the permeate velocity profile can be obtained.

$$\begin{aligned} u_p(x, y) = &\frac{2qk_1k \sinh \frac{y}{q}}{h_p \cosh \frac{w}{q}[k + k_1\omega(c_f + fx)]} \\ &\times \left[\Delta P - \omega c_f + \frac{c_f u_f k_{fb}\mu}{f} \ln \frac{c_f}{c_f + fx} - \omega fx\right] \end{aligned} \tag{10}$$

Downloaded At: 11:38 25 January 2011

RESULTS AND DISCUSSION

Membrane output results are calculated for the 2.5″ modules at particular operating conditions. The dimensions of this type of modules and the numerical values of the characteristic constants of the membrane performance are presented in Table 2. Similar results could be obtained for different operating conditions or geometric configurations. The profile of the effective pressure $\Delta P_{ef}(x, y)$, at real operating conditions, is presented in Fig. 2.

A similar profile will be expected for the water flux through the membrane. It is apparent that the effective pressure and consequently the water flux decrease in the x direction. This is a result of the decreasing applied pressure $P_b(x, y)$ in the brine channel and the increasing salt concentration along the length of the membrane. On the other hand, in the y direction the effective pressure and the water flux increase constantly due to the decreasing pressure $P_p(x, y)$ in the permeate channel. Experimental studies (1) have shown that the permeate pressure $P_p(x, y)$ may vary from 5×10^5 to 1×10^5 Pa. It is interesting that even though the applied pressure is 60×10^5 Pa, the actual driving pressure of the water through the membrane is approximately 22×10^5 Pa. Although one could find useful the profiles of the brine pressure $P_b(x, y)$ and the permeate pressure $P_p(x, y)$, it was thought that this kind of data may be misleading. A high value of the brine pressure does not necessarily mean high water flux, since the salt wall concentration and the permeate pressure should be taken into account.

The plot of Eq. (8) is illustrated in Fig. 3. It must be noted that a constant k value has been assumed along the membrane, although the flow condition vary from point to point. The salt wall concentration increases in both directions x and y. This is a result of the rejection of the salt by the membrane. According to the salt wall concentration profile, the most

TABLE 2
Dimensions of the FT 30 SW 2.5″ Modules and the Values of the Constants for the Membrane Performance

$h_p = 0.43 \times 10^{-3}$ m	$h_b = 0.77 \times 10^{-3}$ m	$h_m = 0.14 \times 10^{-3}$ m
$w = w_{\text{without glue}} = 1.1700$ m	$L = l_{\text{without glue}} = 0.8665$ m	$w_{\text{brine spacer}} = 1.3400$ m
$k = 3.039 \times 10^{-5}$ m/s	$k_1 = 3.815 \times 10^{-12}$ m/s·Pa	$\omega = 728 \times 10^2$ m^3·Pa/kg
$f = 6.05$ kg/m^4	$k_{fb} = 23 \times 10^7$ m^{-2}	$k_{fp} = 11 \times 10^9$ m^{-2}
$P_b(0, \text{for all } y) = 60 \times 10^5$ Pa	$P_p(0, w) = 1 \times 10^5$ Pa	$q = 2.3$ m
$c_b(0, \text{for all } y) = c_f = 35$ kg/m^3	$u_f = 0.1254$ m/s	

Downloaded At: 11:38 25 January 2011

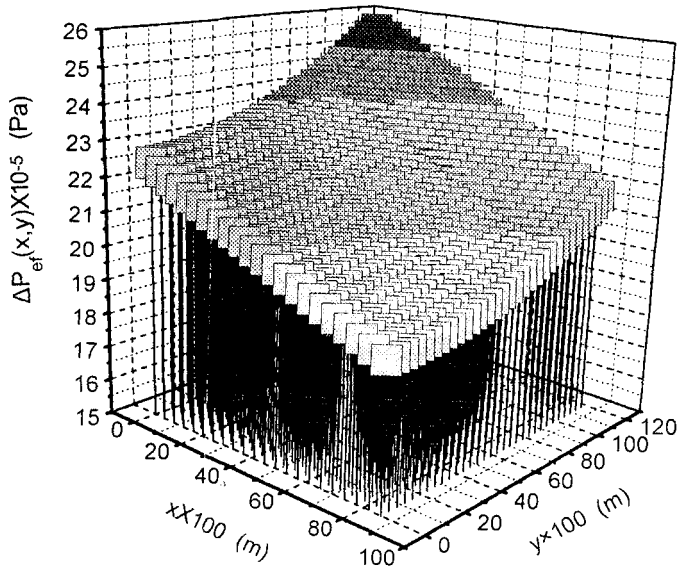

FIG. 2 Effective pressure profile for 35 kg/m^3 seawater solution at 25°C and absolute pressure 60 × 10^5 Pa.

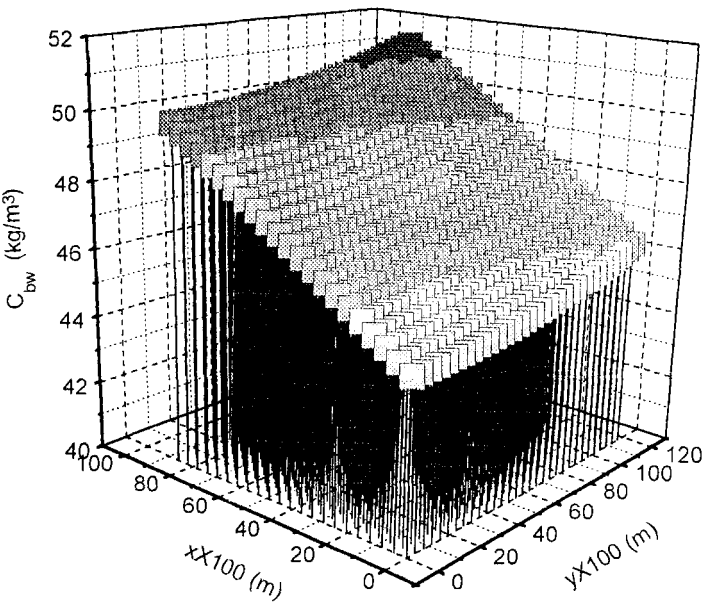

FIG. 3 Salt concentration on the membrane surface for 35 kg/m^3 seawater solution at 25°C and absolute pressure 60 × 10^5 Pa.

Downloaded At: 11:38 25 January 2011

probable point on the membrane surface for salt precipitation is the point (L, w). However, the salt precipitation is not affected only by the concentration of salt but also by other factors, such as the presence of insoluble solids, bubble formation, etc., factors which have been ignored. The maximum salt wall concentration is predicted to be 51.2 kg/m^3 at the particular operating conditions. This leads to a dimensionless concentration ratio at $\alpha = c_{bw}(L, w)/c_f = 1.46$. Sherwood et al. (11) presented a numerical method for the prediction of the salt concentration at the membrane surface. They used seawater membranes at $P_b(0, w) = 100 \times 10^5$ Pa at laminar flow conditions with $u_f = 0.3$ m/s. They concluded that the dimensionless concentration ratio α is 1.6. Additionally they postulated that if osmotic membranes were so improved as to permit a water flux four times as great, the value of the concentration ratio would increase to 5.9 and the recovery ratio R would approach zero.

Similar experiments and numerical calculations for the salt wall concentration were also published by Bhattacharyya et al. (6). However they

Downloaded At: 11:38 25 January 2011

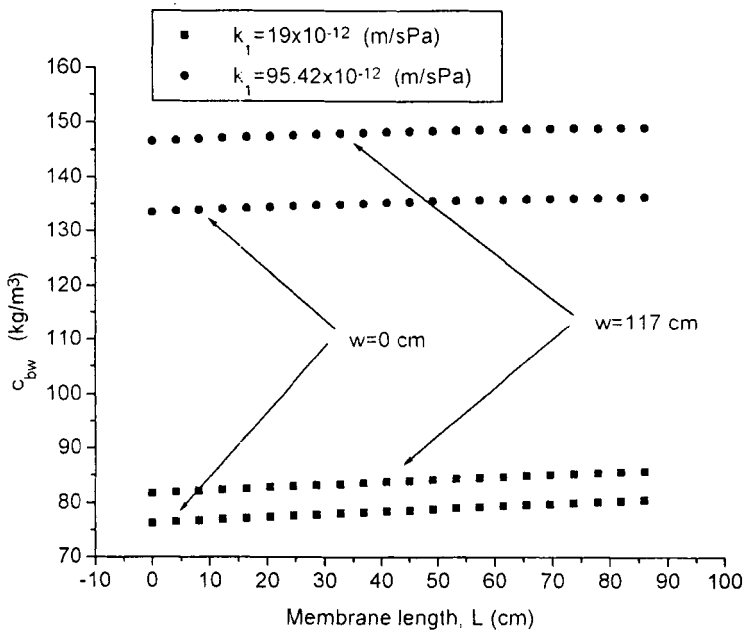

FIG. 4 Hypothetical salt concentration on the membrane surface for 35 kg/m^3 seawater solution at 25°C and absolute pressure from 19 $\times$ 10^5 to 25 $\times$ 10^5 Pa.

used NaCl solutions at a concentration of 5 kg/m^3 and a transmembrane pressure at 30 $\times$ 10^5 Pa. The membrane, on the other hand, was for brackish water with higher permeability properties than the seawater membranes, k_1 = 7.45 $\times$ 10^{-12} m/s·Pa. Their results predict that the salt wall concentration at the exit of the module is four to five times the feed concentration. If the same conclusion is applied for seawater, it is obvious that there would be no water passing through the membrane at this high concentration. As has been concluded in previous work (2), and supported by Sherwood et al. (11), there are doubts about whether the models used for the membrane performance for brackish water can be used for seawater. Nevertheless, if a hypothetical membrane with very high water flux is assumed, then Eq. (8) predicts a very high salt concentration on the membrane surface (see Fig. 4). All the other membrane performance variables were kept constant in the calculations. This means that not only should a very high pressure be applied in order to sustain the recovery ratio, but also scale formation is more likely to occur.

Downloaded At: 11:38 25 January 2011

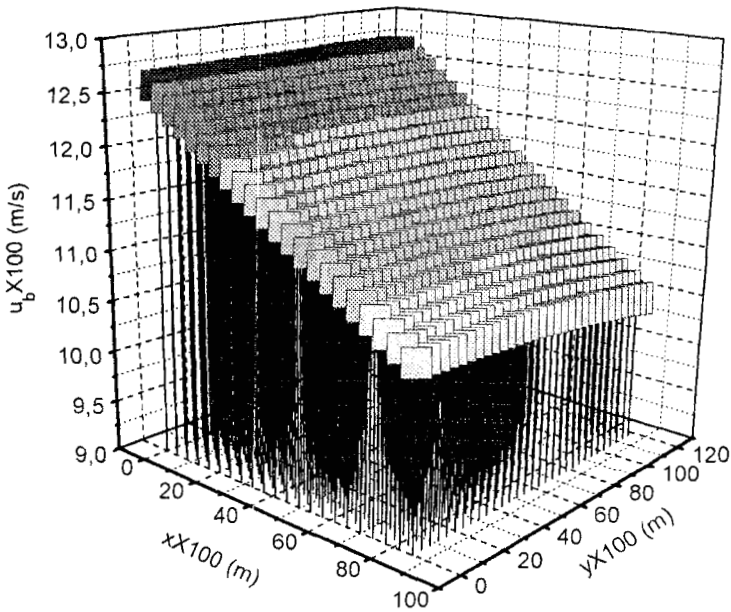

FIG. 5 Brine velocity profile for 35 kg/m^3 seawater solution at 25°C and absolute pressure 60 $\times$ 10^5 Pa.

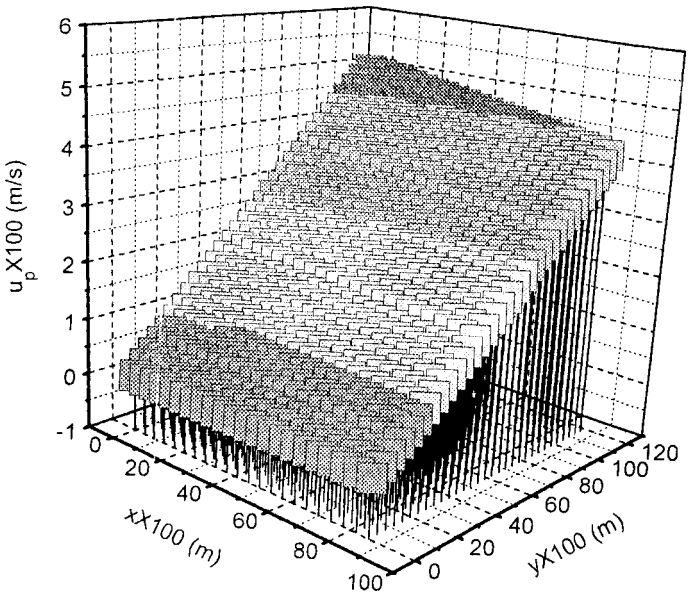

FIG. 6 Permeate velocity profile for 35 kg/m^3 seawater solution at 25°C and absolute pressure 60 × 10^5 Pa.

Downloaded At: 11:38 25 January 2011

The brine velocity decreases in the x direction as a result of the permeation of the water through the membrane (see Fig. 5). On the other hand, the permeate velocity increases in the y direction. In the x direction there are decreases due to the decreasing effective pressure and the water flux in this direction (see Fig. 6). Some characteristic values of all the parameters which have been examined are presented in Table 3.

TABLE 3
Characteristic Values of All Parameters on the Membrane Surface

(x, y) (cm)	$\Delta P_{ef}(x, y)$ (Pa × 10^{-5})	$c_{bw}(x, y)$ (kg/m^3)	$u_b(x, y)$ (m/s)	$u_p(x, y)$ (m/s)
(0, 0)	22.42	44.85	0.1257	0
(0, w)	25.39	46.16	0.1257	0.0486
(L, 0)	19.03	49.82	0.1069	0
(L, w)	21.54	51.1	0.1044	0.0413

CONCLUSIONS

An explicit analytical procedure to determine the flow parameter profiles in the permeate and the brine channel for spiral wound modules has been presented in this work. Although the analytical equations are based on several assumptions, reasonable results have been obtained, and predictions have been made for possible areas where scale formation on the membrane surface could take place. The analysis has shown a clear picture of insight behavior of seawater membranes. The significance of the salt concentration on the membrane surface has been proved. Consequently, the production of seawater membranes with higher permeability properties at reasonable recovery ratios is limited by the cost of energy needed to apply the required pressure and by the undesired scale formation.

SYMBOLS

c	concentration ($kg \cdot m^{-3}$)
ΔP_{ef}	driving pressure (Pa)
ΔP	pressure difference given by $[P_b(0, w) - P_p(0, w)]$ (Pa)
f	concentration gradient coefficient, giving the concentration gradient in the axial direction ($kg \cdot m^{-4}$)
h	height (m)
J	water flux ($m \cdot s^{-1}$)
k	mass transfer coefficient ($m \cdot s^{-1}$)
k_1	water permeability coefficient ($m \cdot s^{-1} \cdot Pa^{-1}$)
k_f	friction parameter (m^{-2})
L	membrane length (axial) (m)
P	pressure (Pa)
q	constant for a given membrane and temperature, defined as $q = \sqrt{\frac{h_p}{2k_1 k_{fp} \mu}}$ (m)
Q	volumetric flow (m^3/s)
R	recovery ratio, defined as $R = Q_p/Q_f$
u	velocity ($m \cdot s^{-1}$)
w	membrane width (tangential) (m)
x	coordinate along the module axis (m)
y	coordinate along the membrane width (m)
(x, y)	any point in the two dimensions plane

Greek Letters

α	dimensionless concentration ratio, defined as $\alpha = c_{bw}(L, w)/c_f$

Downloaded At: 11:38 25 January 2011

μ	viscosity ($kg \cdot m^{-1} \cdot s^{-1}$)
π	osmotic pressure (Pa)
ρ	density ($kg \cdot m^{-3}$)
ω	osmotic pressure coefficient, $\omega = \pi/c$ ($N \cdot m \cdot kg^{-1}$)

Subscripts

b	brine
ef	effective
f	feed
m	membrane
p	permeate
w	wall

REFERENCES

1. S. Avlonitis, W. T. Hanbury, and M. Ben Boudinar, *Desalination*, *82*, 191 (1991).
2. S. Avlonitis, W. T. Hanbury, and M. Ben Boudinar, *Ibid.*, *89*, 227 (1993).
3. A. S. Berman, *J. Appl. Phys.*, *24*(9), 1232 (1953).
4. M. C. Rocco, *3[Drei] R, Rohre, Rohreitungsbau, Rohrleitungstansp.*, *19*, 348 (1980).
5. H. Miyoshi, T. Fukuumoto, and T. Kataoka, *Desalination*, *42*, 47 (1987).
6. D. Bhattacharyya, S. L. Back, and R. I. Kermode, *J. Membr. Sci.*, *48*, 231 (1990).
7. S. Avlonitis, G. P. Sakellaropoulos, and W. T. Hanbury, *Chem. Eng. Res. Design*, *73*(Part A), 575 (1995).
8. R. Rautenbach and W. Dahm, *Desalination*, *65*, 259 (1987).
9. F. Evagelista and G. Jonsson, *Chem. Eng. Commun.*, *72*, 83 (1988).
10. Y. Taniguchi, *Desalination*, *15*, 71 (1978).
11. T. K. Sherwood, P. L. T. Brian, R. E. Fisher, and L. Dresner, *Ind. Eng. Chem. Fundam.*, *4*, 113 (1965).

Received by editor March 9, 1996
Revision received May 22, 1996

Downloaded At: 11:38 25 January 2011